International Journal of Thermal Sciences 91 (2015) 157–166

Contents lists available at ScienceDirect

International Journal of Thermal Sciences

journal homepage: www.elsevier.com/locate/ijts

Local experimental heat transfer of single-phase pulsating laminar flow in a square mini-channel

Balkrishna Mehta, Sameer Khandekar*

Department of Mechanical Engineering, Indian Institute of Technology Kanpur, Kanpur, UP, 208016, India

ARTICLE INFO

Article history:
Received 12 June 2014
Received in revised form
1 January 2015
Accepted 4 January 2015
Available online

Keywords:
Mini-channels
Pulsating flow
Local Nusselt number
Heat transfer enhancement
InfraRed thermography

ABSTRACT

Disturbing a single-phase laminar internal convective flow with a particular pulsating flow frequency alters the thermal and hydrodynamic boundary layer, thus affecting the inter-particle momentum and energy exchange. Due to this externally imposed flow disturbance, augmentation in the heat transfer may be expected. Obviously, parameters like pulsating flow frequency vis-à-vis viscous time scales and the imposed pulsating amplitude will play an important role. Conclusions from reported literature on this and related problems are rather incoherent. Lack of experimental data, especially in micro-/mini internal convective flow situations, with imposed flow pulsations, motivates this study. Non-intrusive infra-red thermography has been utilized to scrutinize heat transfer augmentation during single-phase laminar pulsating flow in a square mini-channel of cross-section 3 mm × 3 mm, electrically heated from one side by a thin SS strip heater (70 μm, negligible thermal inertia); all the other three sides of the channel are insulated. The study is done at different pulsating flow frequencies of 0.05 Hz, 1.00 Hz and 3.00 Hz (Wo = 0.8, 3.4 and 5.9, respectively). These values are chosen because pulsatile velocity profiles exhibit different characteristics for $Wo > 1$ (annular effect, i.e., peak velocity near the channel walls) and $Wo < 1$ (conventional parabolic profile). Local streamwise heat transfer coefficient has been determined using the time averaged spatial IR thermograms of the heater surface and the local fluid temperature, linearly interpolated from measured value of inlet and outlet bulk mean mixing temperature. It is observed that for measured frequency range, the overall enhancement in the heat transfer is not attractive for laminar pulsating flow in comparison to steady flow with same time-averaged flow Reynolds number. The change is either marginal or highly limited, primarily occurring in the developing length of the channel. Thus, the results suggest that heat transfer enhancement due to periodic pulsating flow is questionable, and at best, rather limited.

1. Introduction

Single-phase fluid flow and heat transfer in pulsating flows are encountered in many engineering systems, ranging from industrial applications like electronics cooling, certain heat exchangers, pulse-tube cooling systems etc., to biological applications of arterial blood flow. The flow pulsations or fluctuations may sometimes be inherent to the flow situation (flow over tube bundles where vortex shedding from the leading tube induces fluctuations for subsequent tubes) or it may be externally superimposed on a steady flow (e.g., in a pulsed-jet situation). Cooling requirements in contemporary are significantly increasing due to the miniaturization of the engineering devices and increasing heat flux handling requirements. MEMS and Bio-fluidic systems are also gaining popularity, which may also encounter pulsatile flows with simultaneous heat/mass transfer. The explicit effect of pulsations on local and average heat transfer in internal convective is an interesting problem *per se* due to several complexities involved.

Several researchers have been working towards finding the insights of pulsatile flows from early decades of the last century. In a classical study Richardson and Tyler [1], experimentally discovered that pulsating flow field in circular, square and oval cross section tubes may lead to the 'annular effect' i.e., under certain operating flow conditions, the maximum velocity at the channel cross-section occurs near the tube wall and not at its center. Several others [2–4] studied oscillating flows in arterial systems to observe the differences in the manifested velocity distribution and viscous drag in comparison to a steady laminar flow. Uchida [5] theoretically studied the hydrodynamics of pulsating flow in circular tube for different non-dimensional frequencies and established that

* Corresponding author. Tel.: +91 512 259 7038; fax: +91 512 259 7408.
E-mail address: samkhan@iitk.ac.in (S. Khandekar).

http://dx.doi.org/10.1016/j.ijthermalsci.2015.01.008
1290-0729/

Nomenclature

A	amplitude ratio ($\lvert U_t/U_{av}\rvert = \lvert Q_i^* - 1\rvert$) (−)
Bi	Biot number ($h \cdot L_c/k_w$) (−)
D	diameter (m)
f	frequency of pulsation (Hz)
Fo	Fourier number ($\alpha \cdot t/L_c^2$) (−)
h	heat transfer coefficient (W/m^2 K)
k	thermal conductivity (W/m K)
L	length (m)
Nu	Nusselt number ($h \cdot D_h/k$) (−)
Pr	Prandtl number (υ/α) (−)
Q	volumetric flow rate ($Q_t + Q_{av}$) (m^3/s)
Q_i^*	instantaneous flow rate ratio (Q/Q_{av}) (−)
q″	heat flux (W/m^2)
Re	Reynolds number ($U_{av} \cdot D_h/\upsilon$) (−)
St	Strouhal number ($f \cdot D_h/U_{av}$) (−)
t^*	non-dimensional time (t/θ) (−)
T^*	non-dimensional temperature (−)
U	axial flow velocity ($U = U_{av} \pm U_t$) (m/s)
Wo	Womersley number ($d \cdot (\omega/\upsilon)^{0.5}$) = ($2\pi \cdot St \cdot Re$)$^{0.5}$ (−)
z	axial length (m)
Z^*	non-dimensional axial length ($z/Re \cdot Pr \cdot D_h$) (−)

Greek symbols

α	thermal diffusivity (m^2/s)
υ	kinematic viscosity (m^2/s)
ω	angular frequency (rad/s)
θ	time period (s)

Subscripts

av	average
c	characteristic
f	fluid
h	hydraulic, hydrodynamic
i	instantaneous
in	inlet
r	relative
s	steady state
t	transient/unsteady component
w	wall
*	non-dimensional quantity

phase-lag between the pressure gradient and velocity increases with frequency and this lag asymptotically approaches to 90° for infinite frequency of flow oscillations. Yakhot et al. [6] numerically analyzed pulsating laminar flow of a viscous, incompressible liquid in a rectangular duct. It was concluded that at low imposed frequencies, practically no phase-lag existed between the pressure gradient and resulting velocities, but, at higher frequencies, phase-lag increased.

More recently, Chang et al. [7] have made another attempt to analyze the phase-lag between the imposed pressure gradient and flow rate in low frequency laminar pulsating flow. This study concluded that phase-lag exists even at very low frequency (less than 0.5 Hz) in laminar pulsating flow through circular pipes and parallel plate. Phase-lag increases with increase in frequency and hydraulic diameter of the tube/duct, but decreases with increase in viscosity and remained unaffected by the applied pulsation amplitude. Ray et al. [8], carried out extensive numerical simulations and obtained a correlation to predict the development length for laminar, developing flow through pipes under sinusoidally varying mass flow rate. Computations were done for moderate to high mean flow Reynolds number region ($100 \leq Re_{av} \leq 2000$), dimensionless amplitude of mass flow rate pulsations of 0.2, 0.4 and 0.8 (i.e. ratio of amplitude of mass flow rate pulsations to the time averaged mass flow rate in the channel) values and non-dimensional frequency parameter was varied from 0.1 to 20 i.e., complete region from quasi-steady to inertia-dominant region was covered in this study. It was found that at low imposed flow frequency, variation in the instantaneous development length is sinusoidal and can be predicted from the steady state flow condition based on instantaneous flow *Re*. On the other hand, when frequency of pulsation is higher, amplitude of the development length decreases; therefore, estimation of maximum flow development length based on maximum *Re* will give the most conservative estimate. Normalized variation of development length has been found to be independent of average Reynolds number Re_{av}, but it depends on non-dimensional frequency and mass flow rate amplitude ratios.

Siegel and Perlmutter [9] have shown the dependence of overall heat transfer on the frequency of pulsations. Furthermore, when constant temperature wall boundary condition was used, the Nusselt number showed periodic fluctuations along the flow direction. In other subsequent studies [10–15], hydrodynamic 'annular effect', phase-lag and periodic axial fluctuation of fluid temperature and heat transfer were confirmed. However, Seigel [16] argued that, for forced convection in laminar flow in a channel, flow oscillations tend to reduce the heat transfer coefficient. Cho and Hyun [17], numerically investigated the effect of flow pulsations in a pipe using laminar boundary layer equations. It was observed that at the fully developed downstream region, Nusselt number may increase or decrease depending on the frequency parameter (*Wo*). Kim et al. [18] studied the thermally developing but hydrodynamically fully-developed pulsating channel flow and isothermal channel walls. They observed that flow pulsations hardly affected the thermal behavior. Guo and Sung [19] observed that for small amplitudes, heat transfer gets augmented within a band of operating frequencies but at higher amplitudes, heat transfer gets always augmented. Hemida et al. [20] observed that pulsations produced little changes in heat transfer, the change being always negative. In addition, this small change is limited to the thermally developing region only. Jun et al. [21], executed an experimental study to understand heat transfer characteristics of pulsating flow and concluded that by increasing the flow rate, heat transfer gradually increases and strong pulsations result in enhancement of heat transfer. However, in this study, there were some measurement ambiguities, e.g., (a) heat transfer estimations were averaged out in space and time (b) heat balance has been done based on local fluid measurements by thermocouples, which measure the local instantaneous temperature but not the bulk mean mixing temperature (c) Non-dimensional parameterization has not been done, which make the interpretation of results non-universal and confined to the reported study only. Yu et al. [22] and Chattopadhyay et al. [23] observed no change in time-averaged Nusselt number due to flow pulsations. Bouvier et al. [24], performed an experimental study to understand heat transfer in oscillating flow in a circular pipe. Parameters used in this study were maximum Reynolds number, non-dimensional frequency (*Wo*) and amplitude of oscillation. Temperatures were measured inside the fluid and at different radial locations at the wall and heat

transfer has been estimated from these measurements. Fundamental frequencies of the transient temperature data obtained from wall and the fluid were not identical due to the thermal inertia of the pipe wall. Nield and Kuznetsov [25] used a perturbation technique to obtain the analytical expression for velocity, temperature and transient Nusselt number for pressure gradient governed pulsating flow in parallel plate channel or inside a circular tube. Uniform heat flux condition was used at the wall. Axial conduction, either in the fluid or in the wall was neglected. It was found that Nusselt number is dependent on the frequency of the fluctuating part and the *Pr*. As the *Pr* increases, amplitude of fluctuating *Nu* goes down. For a fixed *Pr*, with increase in imposed flow frequency, *Nu* first increases and then after achieving its maximum, it again gets reduced. Mehta and Khandekar [26] presented a numerical study of hydrodynamics and heat transfer of pulsating channel flow by applying a sinusoidal velocity profile at the channel inlet. Here too, it was observed that pulsations hardly affected the local distribution of axial heat transfer. Similar numerical simulations done with simple fluids and nano-fluids also show no specific advantage of using imposed flow pulsations for average heat transfer enhancement [27].

It is clear that available literature does not converge to coherent conclusions. The results are not only sparse but inconsistent and sometimes contradictory. The key issue concerning heat transfer in pulsating internal convection is whether the superposed flow pulsations enhance heat transfer as compared to the original steady flow. Unfortunately, the literature provides diverging answers, i.e., (a) pulsations enhance heat transfer [28]; (b) it deteriorates the heat transfer [20]; (c) it does not affect the heat transfer [9,22,23,26]; (d) it either increases or deteriorates the heat transfer depending on imposed flow parameters [18,19]. The literature also lacks in systematic experimental data, especially for mini-/micro scale geometries. This situation necessitates careful non-intrusive and methodical experimental studies to discern the explicit effect of pulsations on local heat transfer.

In this background, we have attempted to experimentally investigate heat transfer during internal convective laminar flow with imposed flow rate pulsations in a horizontal square mini-channel of cross-section 3 mm × 3 mm under constant heat flux condition applied to one wall. Fig. 1(a)-(i–iii) shows the schematic representation of different types of pulsating and oscillating flow waveform. The term 'pulsating flow' (shown in Fig. 1(a)-(i)) is used when flow is transient and unidirectional, i.e., non-zero mean flow while 'oscillating flow' (shown in Fig. 1(a)-(ii)) is used when flow changes its direction, i.e., zero mean flow. Fig. 1(a)-(iii) shows a specific type of pulsating flow where it is always unidirectional but the minimum flow is zero. In the present work, this latter type of pulsating flow condition is generated by using solenoid valves, though the flow waveform is not sinusoidal but close to square wave, as will be discussed later. The experimental arrangement is such the flow would have been hydrodynamically fully developed and thermally developing, if the imposed pulsations were not present. Distinct flow rate pulsations have been incorporated, keeping the average flow Reynolds number to be constant.

2. Experimental details and data reduction

The schematic and dimensional detail of experimental setup is shown in Fig. 1(b). A square channel of cross-section size 3 mm × 3 mm is machined on 500 mm × 250 mm × 12 mm

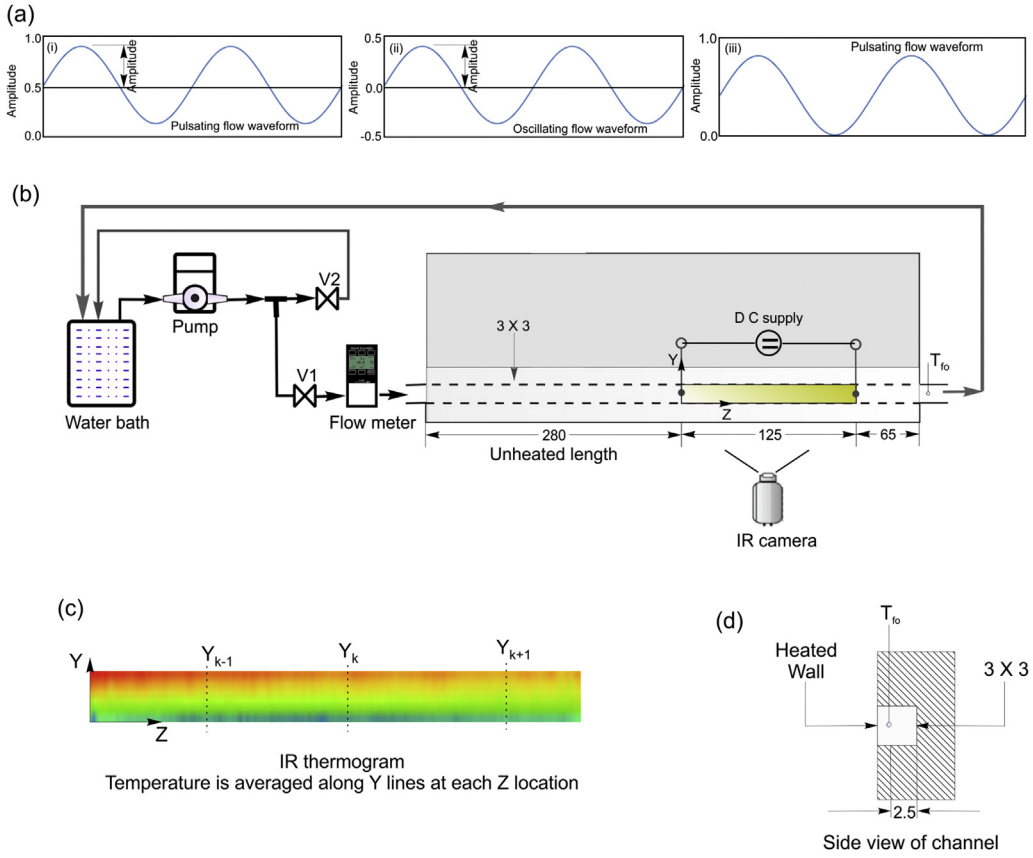

Fig. 1. (a) Schematic showing difference in pulsating and oscillating flow (b) Schematic and dimensional details of the experimental set-up (c) Averaging scheme of wall temperature in Y direction (d) Enlarged view of the channel cross-section.

polycarbonate substrate. An unheated length of 280 mm is provided for the hydrodynamic development of the flow. The heated length is kept as 125 mm and another unheated 65 mm length is provided after the heater to minimize the end effects in the heated test section. The strip heater is made of 70 μm thin SS strip. 150 mm long and 4 mm wide SS strip is attached over the polycarbonate square channel such that heater itself will act as fourth wall of the channel, the three remaining walls being cut in the polycarbonate material, as noted earlier, and therefore they remain insulated (refer Fig. 1(d)). Heater strip is heated by Joule heating using a high current DC power supply (V: 0–60 V and I: 0–50 A) which ensures the constant heat flux thermal boundary condition. As the thickness of the heated wall is only 70 microns, even with assuming a large value of h, say, 1000 W/m^2 K, the corresponding value of the Biot number $Bi = hL_c/k_w << 0.004$, clearly suggesting that the heater wall is thin enough so that its outer surface temperature can be effectively taken to be equal to the temperature of fluid-wall interface. In addition, the pulsating frequency used in the experiments are 0.05 Hz, 1 Hz and 3.0 Hz, corresponding to non-dimensional frequency parameter $Wo = 0.8$, 3.4 and 5.9, respectively (alternately, Strouhal number (St) can also be used, which only includes geometric and frequency parameter). Thus, diffusional time constant in the Fourier number ($Fo = \alpha \cdot t/L_c^2$), is the order of 10^{-3}, respectively. Heat capacity of the heater is equal to 0.15 J/K. Therefore, it is safe to assume that there is negligible transverse temperature gradient as well as no significant signal lag in the transverse direction of the thin heater strip. The outer wall temperature of the heater is imaged by IR camera and one thermocouple (Make: Omega®) of bead diameter 0.13 mm has been inserted in fluid domain at the outlet, located as shown in Fig. 1(b).

De-ionized and de-gassed water at constant temperature from thermal bath (Make: Julabo® F34 ME, accuracy ± 0.1 K) is supplied in the square mini-channel. A flow meter with a time response of 20 ms (Make: Cole-Parmer®; L-series; laminar-orifice Poiseuille flow meter) is used to measure the transient liquid flow rate. The imposed flow pulsations are created by two electronically controlled solenoid valves V1 and V2 (Make: Burkert®), as shown in Fig. 1(b). The pulsed flow is generated by alternately opening the two valves, i.e., there will be a flow in the test section for half time period and no flow in the next half of the time period. Thus, the flow in the test section will result in a near-square waveform. In this work, three imposed flow frequencies have been used, 0.05 Hz, 1.0 Hz and 3.0 Hz. In all the experiments, the flow amplitude ratio ($A = |Q_i^* - 1|$), defined as ratio of peak value of fluctuating component of velocity to the time-averaged value of the flow velocity, is fixed, and is close to the value of 0.92. Theoretically, this value should be equal to unity for a pure square waveform, which varies between zero and a maximum peak value. However, in the present case, the experimentally obtained waveform somewhat deviates from this ideal situation due to mechanical inertia of the solenoid valves (as will seen in the next section). The average Reynolds number of the flow, at all the imposed frequencies, is fixed at 170.

An IR camera with an operational spectral band of 3–5 μm, 14 bit signal digitization and a Noise Equivalent Temperature Difference of less than 0.02 K at 30 °C, is used to measure the wall temperature (Make: FLIR®, Model: SC4000; Indium Antimonide detector array). ThermaCAM™ Researcher V-2.9 is used to acquire the images from IR camera. Acquisition rate has been kept at 20 Hz and IR thermograms are captured at 320 pixels × 256 pixels (105 mm × 96 mm) which gives a spatial resolution of 330 microns in the axial z-direction and 375 microns in the transverse y-direction, on the heated thin wall. NI-cDAQ 9172 with NI 9205 module and NI-USB 9162 (Make: National Instruments®) cards are used to acquire the voltage signal from flow meter and fluid thermocouple temperature located at the outlet, respectively. These acquisitions are also done at 20 Hz.

2.1. Data reduction

As noted above, the primary data collected is the spatio-temporal IR thermogram of the heated wall and the bulk mean mixing fluid temperature at the inlet and outlet of the channel obtained by respective thermocouples. From this primary data, the time averaged Nusselt number is calculated as follows:

$$Nu_{ta} = \frac{q'' \cdot D_h}{\left(\overline{T}_w - \overline{T}_b\right)_{ta} \cdot k_f} \tag{1}$$

$\overline{T}_w$ = local wall temperature at any given location along the z-axis, averaged along the direction of Y-axis, as shown in Fig. 1(c).
$\overline{T}_b$ = local bulk mean mixing temperature of the fluid estimated by linear interpolation of measured temperature by the thermocouples at the flow inlet and outlet cross section of the channel, respectively.

$$T^* = \frac{\left(T - T_{f,in}\right)}{q'' \cdot D_h \Big/ k_f} \tag{2}$$

It must be noted that local measurement of the bulk mean mixing temperature of the fluid, $\overline{T}_b$, under pulsatile conditions is not trivial. Especially when the flow is in mini/microscale geometries, non-intrusive techniques for the temperature measurement of the fluid domain must be employed. In the absence of this local experimental data for $\overline{T}_b$, from a global energy balance point of view, the best available option is averaging of the inlet and outlet bulk mean mixing temperatures of the fluid. While this approach has limitations, however, as will be seen later, it does give a fairly good insight of the overall thermal transport characteristics.

3. Results and discussion

In this type of flow, parameters like pulsating flow frequency vis-à-vis viscous time scales and the imposed pulsating amplitude play an important role. The present study is done at three different pulsating flow-rate frequencies of 0.05 Hz, 1.0 Hz and 3.0 Hz, respectively (Womersley number Wo = 0.8, 3.4 and 5.9). These values are chosen because, as per the established literature, pulsatile velocity profiles exhibit distinctly different characteristics for $Wo > 1$ (annular effect, i.e., peak velocity occurs near the channel walls) and $Wo < 1$ (conventional parabolic velocity profile) [29]. Due to transient nature of the flow, different time scales are involved which govern the evolution of the thermal field. These time scales are: fluid thermal diffusion time scale (D^2/α), imposed time-period of flow fluctuations ($1/f$), convective time scale (L_h/U_{av}) and thermal diffusion time scale in the heater (L_c^2/α). The values of these time scales are shown in Table 1 for Wo = 0.8, 3.4 and 5.9, respectively. It can be seen that for all imposed frequencies,

Table 1
Different experimental time scales.

Time scale (s)	$Wo = 0.8$	$Wo = 3.4$	$Wo = 5.9$
Imposed time scale, $1/f$	20	1	0.333
Diffusion in fluid, D^2/α	64	64	64
Diffusion in heater wall, L_c^2/α	0.0009	0.0009	0.0009
Convective time scale, L_h/U_{av}	1.875	1.875	1.875

diffusion in the heater is quite fast to justify the assumption of 'near instantaneous' thermal response, as captured by the IR camera. In other words, the thermal fluctuations experienced by the heater towards the fluid–solid interaction face are well captured at the opposite face, which is exposed to the IR camera (refer Fig. 1(b)). As noted earlier, for direct comparative study, the imposed convective time scale, based on average flow velocity, has been kept identical for all the operating frequencies.

In this background, waveform of instantaneous flow rate ratio and the corresponding variation of non-dimensional local fluid temperature at outlet of the channel acquired by the thermocouple and frequency spectrum from both the signals are shown in Fig. 2(a–f), for the applied frequencies of $Wo = 0.8$, 3.4 and 5.9, respectively. It can be observed that waveform pattern of the flow is close to a square wave, increasing pulsating flow frequency bringing some minor deviations due to mechanical response of the solenoid valve arrangement. For a complete cycle, flow takes place for half of the cycle ('on-cycle') and no flow occurs in the other half of cycle ('off-cycle'). Due to such type of imposed flow pulsations, average fluid temperature at any location oscillates in a periodic manner, decreasing in the 'on-cycle' and increasing in the 'off-cycle'. The time duration, and hence the flow frequency of the 'on-cycle' and the 'off-cycle' is controlled by the solenoid valve arrangement.

At low operating frequency, more time is available for diffusional heat transfer during the 'stop-over' cycle time, as seen from Table 1. This is clearly seen in Fig. 2(a), wherein, as the half-time period of oscillation is 10 s ($f = 0.05$ Hz), there is sufficient time when 'no-flow' conditions exist in the channel, and hence, significant amount of heat is conducted to the fluid by the constant heat flux heater wall, which eventually increases its temperature. A conduction-type boundary layer gets formed during the 'no-

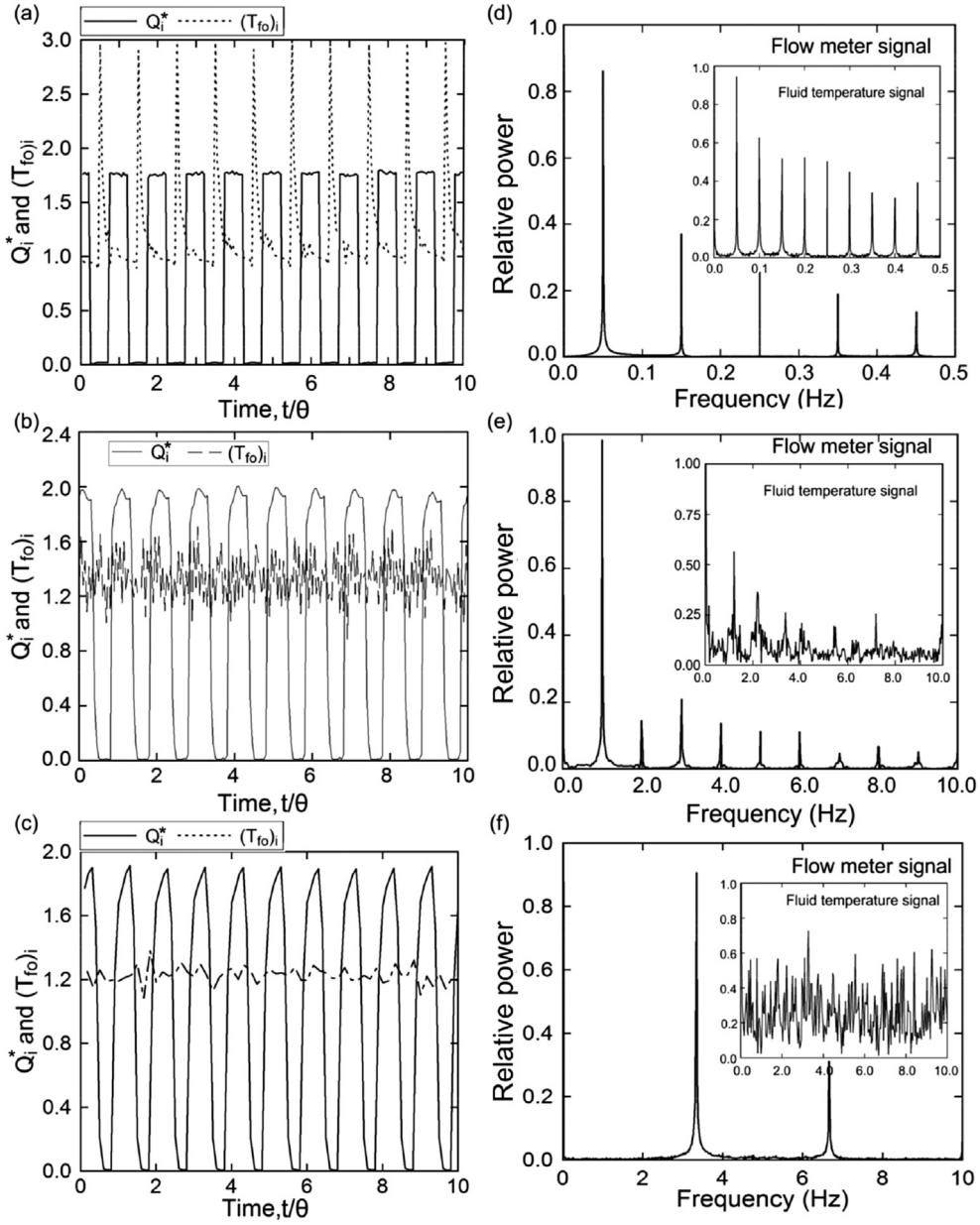

Fig. 2. (a), (b) and (c) show the time variation of non-dimensional instantaneous liquid flow rate ratio and non-dimensional fluid temperature for $Wo = 0.8$, 3.4 and 5.9 respectively; (d), (e) and (f) show the corresponding FFT of flow meter signal and outlet fluid thermocouple signal, respectively.

flow' stage which gets convected when flow resumes in the next half-cycle. At the higher imposed flow frequency, convection continues to be dominant as available diffusional time-period is considerably smaller. As can be seen, in Fig. 2(b) and (c) for $Wo = 3.4$ and 5.9, convection is dominant which resulted in overall low value of local outlet fluid temperature, in contrast to the former case of $Wo = 0.8$. A direct outcome of the available scaling between convective time and diffusive time also leads to the fact that oscillating amplitude of the local outlet fluid temperature is considerably higher and well-structured for $Wo = 0.8$, while for $Wo = 3.4$ and 5.9, local outlet fluid temperature oscillations are quite weak. This fact is highlighted by plotting the power spectrum of the flow meter signal and the local outlet fluid temperature (in the inset), as shown in Fig. 2(d) (e) and (f), respectively, at the corresponding operating frequencies. It can be verified that the dominant frequency of oscillation of the local outlet fluid temperature is identical to the imposed flow frequency, in all the cases.

Fig. 3(a–b) shows the temporal variation of line averaged wall temperatures (averaged in the transverse Y-direction) acquired by IRT at three different axial locations ($Z^* = 0.014$, 0.034 and 0.054). The corresponding frequency spectrum, for $Wo = 0.8$ and 3.4, is shown alongside in Fig. 3(c–d), respectively. It can be observed that for $Wo = 0.8$, fluctuations in wall temperature are clearly observable and patterns are well-structured at all the three axial locations. The relative amplitude of the power spectrum is also nearly identical for all the three downstream locations. This is because, at such low pulsation frequency, the flow and thermal fields have sufficient time to respond according to the imposed disturbances, due to comparatively low wall thermal inertia. In contrast, for $Wo = 3.4$, well-structured fluctuation patterns of local wall temperature are only observed close to the channel inlet; the corresponding amplitudes of wall temperature fluctuation are also less. At far downstream locations, fluctuations are random and no characteristic frequency is observed, as evident from Fig. 3(c) and (d). This occurs mainly because the disturbances created by the imposed pulsation get attenuated by viscous force of the fluid during its motion. At the same time, when imposed flow frequencies exceed the transverse diffusional frequencies, the heater wall will tend to remain isolated from the thermal disturbances occurring in the fluid core region.

Fig. 4(a–c) shows the axial variation of heater wall temperature during the first-half cycle ('off-cycle' represented by $[t_{1/2}]_A$) and the second half-cycle ('on-cycle' represented by $[t_{1/2}]_B$) for $Wo = 0.8$ and corresponding thermograms at various instants. In Fig. 4(a), one complete cycle is shown with the time instants at which thermograms and axial temperature profile are reported. Fig. 4(b–c) depicts the IR thermogram and axial temperature profile for 'on-cycle' and 'off-cycle', respectively. It can be observed that during 'on-cycle' the fluid flow fully establishes in the heated zone while in the 'off-cycle' the fluid flow essentially stops. In the entire cycle, heat is continuously coming in by the heated wall and the channel remains filled up with the working fluid. The incoming heat gets convected in the 'on cycle' by the flowing fluid

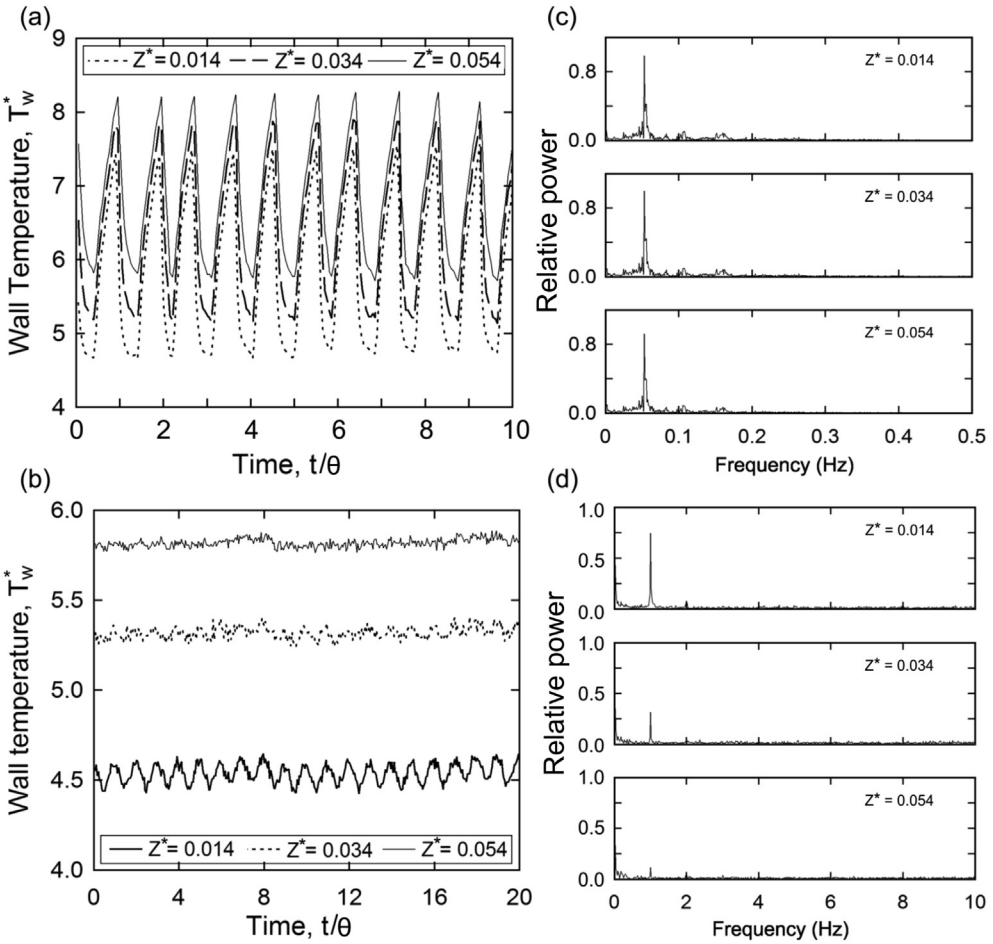

Fig. 3. Temporal variation of wall temperature at different axial locations for (a) $Wo = 0.8$ (b) $Wo = 3.4$ and the corresponding FFT (c) $Wo = 0.8$ (d) $Wo = 3.4$, respectively.

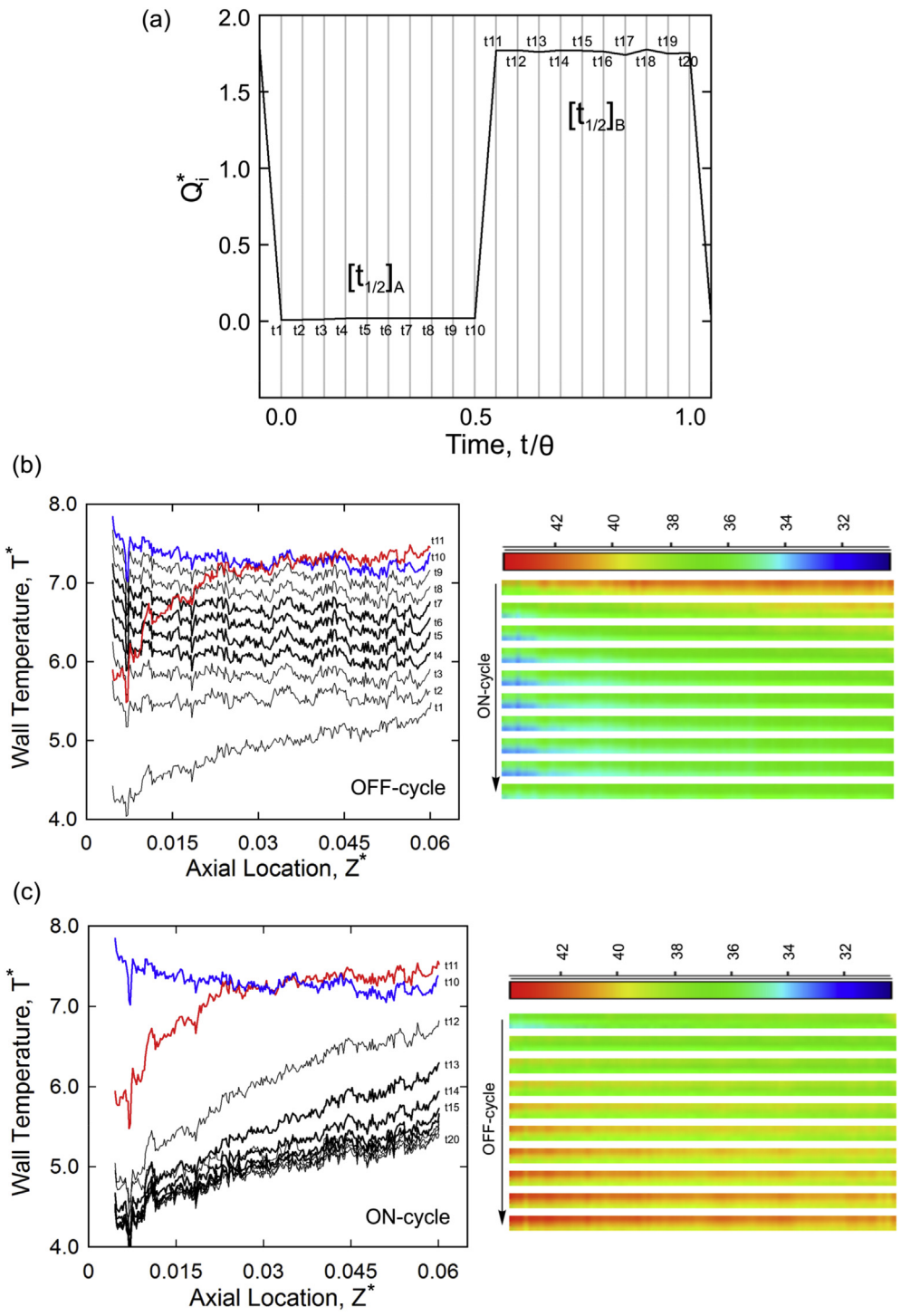

Fig. 4. (a) Different time instants shown on one complete flow cycle (b) Axial wall temperature at various instants and IR thermograms during 'off-cycle' for $Wo = 0.8$ (c) Axial wall temperature at various instants and IR thermograms during 'on-cycle' for $Wo = 0.8$.

but in the 'off-cycle', only diffusional heat transfer from the heater wall to the fluid is possible. As discussed earlier, the thermal response of the heated wall will depend on the available time scales for these two processes (axial convection and transverse diffusion), which eventually is guided by the imposed flow frequency. It can be clearly seen that at lower frequency $Wo = 0.8$, wall temperature is high because of its higher residence time in the heated zone during the 'off-cycle'. Wall temperature distribution approximately becomes axially constant due to dominance of diffusion in the fluid. As the uniform heat flux is applied at heated wall, therefore it is expected that fluid bulk mean temperature will also be approximately axially constant. On the other hand, during the 'on-cycle', when fluid flow starts in the channel, convection dominates and wall temperature gradually decreases with the establishment of convective flow and takes the axially increasing trend as observed in steady uniform heat flux case.

Similarly, axial variation of wall temperature and IR thermogram is presented as shown above in Fig. 5, during the complete

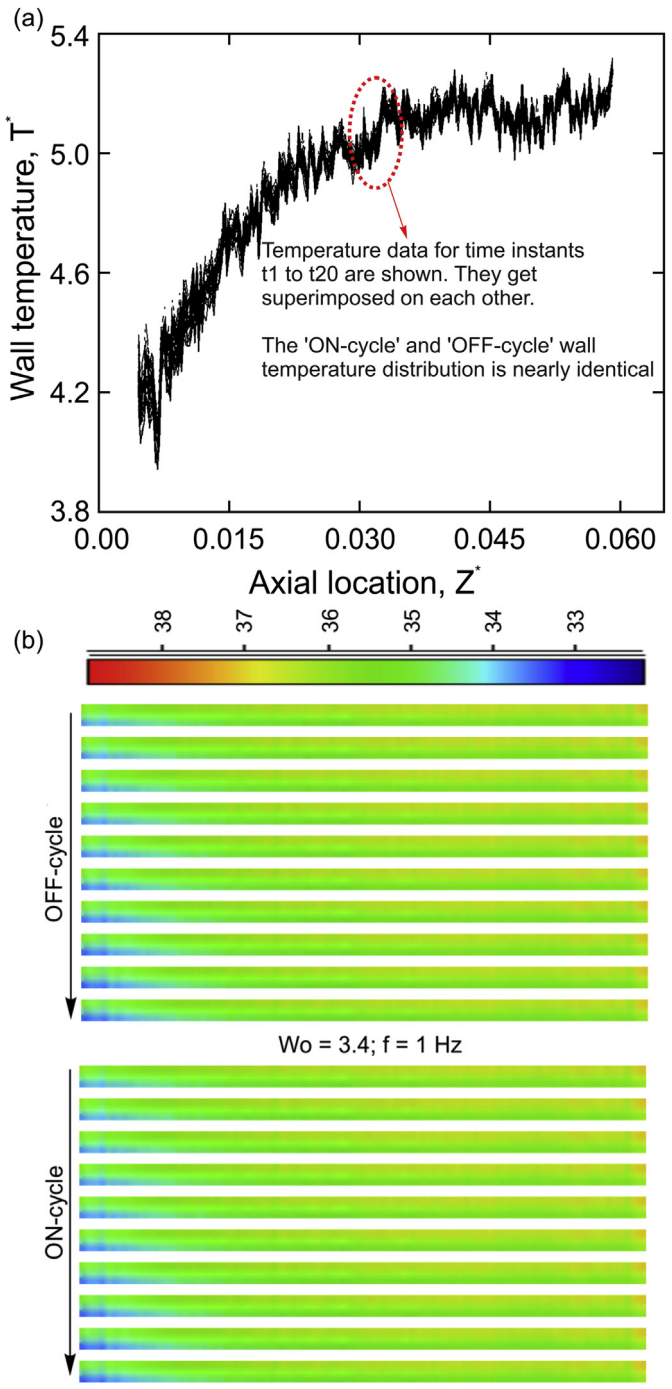

Fig. 5. (a) Axial variation of wall temperature (b) IR thermogram at various time instants of a complete cycle for $Wo = 3.4$.

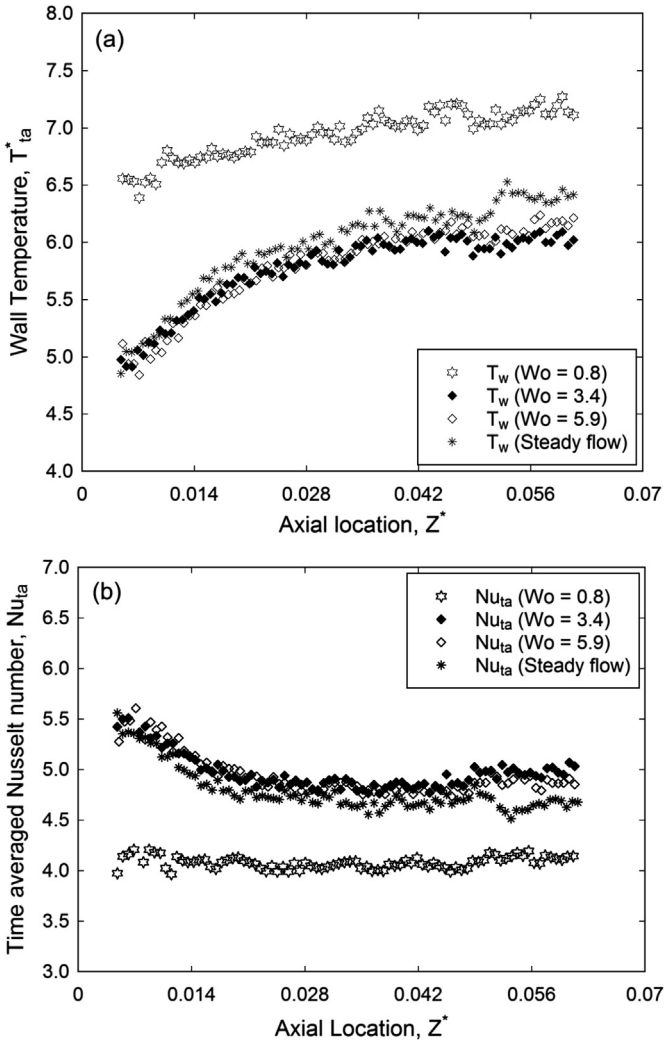

Fig. 6. (a) Axial variation of wall temperature for steady and pulsating flow for $Wo = 0.8$, 3.4 and 5.9 (b) Corresponding axial variation of time averaged Nusselt number for steady and pulsating flow.

cycle for $Wo = 3.4$. The contrast between Fig. 4(b, c) and Fig. 5(a) is worth noting. Here, it is observed that effect of diffusion is not significant because the stop-over time between the 'off-cycle' and 'on-cycle' is very less as compared to the earlier case of $Wo = 0.8$. It is clear from Table 1 that convective time scale is higher than the imposed time scale, i.e., the fluid particle that enters in the heated zone cannot cross it completely in one cycle of imposed fluctuation. Fluid, which is under convection during the 'on-cycle', resides in the heated zone, i.e., fluid particle does not completely come out of the heated zone during the 'on-cycle'. Therefore, the effect of diffusion is insignificant for the higher frequencies. It means that the flow at higher imposed flow frequencies tends to behave more closely like a steady flow situation. Qualitatively, similar results (as for $Wo = 3.4$) are obtained for the higher operating frequency ($Wo = 5.9$) also.

Next, to get the overall picture of imposed pulsations on wall temperature for the same time averaged flow rate and amplitude ratio, axial distribution of time-averaged wall temperatures is plotted for different frequencies in Fig. 6(a). It is observed that for $Wo = 0.8$, time-averaged wall temperature is higher than the steady flow. Isothermalization of wall temperature is also clearly visible here. This is mainly due to the dominance of transverse diffusional heat transfer (no convective heat transfer) during the 'off-cycle', which cannot be completely recovered by the convective flow during 'on-cycle'. Unlike the case of $Wo = 0.8$, axial variation of time averaged wall temperature is similar to the steady-state temperature profile for $Wo = 3.4$ and 5.9, i.e., convection is dominant. In the laminar internal convective flows with uniform wall heating case, transverse exchange of energy largely depends on near wall transverse diffusion while convection is dominant in the axial direction. Therefore, pulsating flows can only enhance heat transfer in systems where transverse exchange of heat is somehow augmented (For example, turbulent flows or fluids with lower

Prandtl number are better candidates for getting augmented heat transfer with pulsating flows-this fact is corroborated by the literature [30]). Hence, it is seen that, no significant effect of imposed pulsations is observed on the temperature profile for the present experiment.

Finally, all the above analysis will be concluded by estimating the enhancement/deterioration of the time-averaged *Nu* due to application of flow pulsations. In Fig. 6(b), axial variation of time averaged Nusselt number is shown for steady-state and pulsating flow at all the frequencies. It is observed that time averaged Nusselt number for $Wo = 0.8$ is lower than the steady-state value. On the other hand, for $Wo = 3.4$ and 5.9, *Nu* shows marginal enhancement over corresponding steady-state value, as expected.

Next, we compare our heat transfer results with some comprehensive contemporary studies reported in the literature. The non-conclusive nature of the reported literature about heat transfer augmentation by pulsatile flows has been discussed earlier. Hemida et al. [20] explicitly concluded that no enhancement in the Nusselt number is possible by imposed flow pulsations, either in fully developed flow or in thermally developing region. On the other hand, Brereton and Jiang [31] show that enhancement and deterioration in mean Nusselt number is conditional, depending on the flow parameters, as well as the type of the externally applied pulsating waveform. The results of Hemida et al. [20] and Brereton and Jiang [31], with the respective flow conditions, are shown in Fig. 7; for the latter case, the two waveforms resulting in enhancement and deterioration respectively, is also shown alongside. The results from the present study are also shown here for a range of *Wo* (detailed results and analysis of only three frequencies, $Wo = 0.8$, 3.4 and 5.9 were reported earlier, however, several tests at other *Wo* were also conducted; this figure provides comprehensive data).

The order of magnitude of enhancement obtained in the present study is comparable to that of Brereton and Jiang [31]. The qualitative nature of the waveform from which Brereton and Jiang [31] got enhancement is also similar to the present waveform. However, in contrast to the thermally developed flow of Brereton and Jiang [31], the present experiments report thermally developing flow. Below *Wo* ~1.5, a deterioration in *Nu* was observed in the present experiments. From a time-scaling perspective, it is logical to assume that the diffusional and thermal time scale (represented by the Prandtl number) must interact with the other relevant time scales which affect the local as well as global time and space averaged *Nu*. Unfortunately, a large experimental database of the explicit effect of *Pr* on *Nu* is not available for pulsatile flows, although analytical/numerical studies of Hemida et al. [20] and Brereton and Jiang [31] do provide some broad hints. Logical extension of Fig. 7 ought to include a power law relation between $(Wo \cdot Pr)$ and *Nu*. However, this relationship may eventually turn out to be so complex and elusive that Brereton and Jiang [31] conclude by noting that modeling the *Nu* as power-law function of *Pr* is pointless in transient flows.

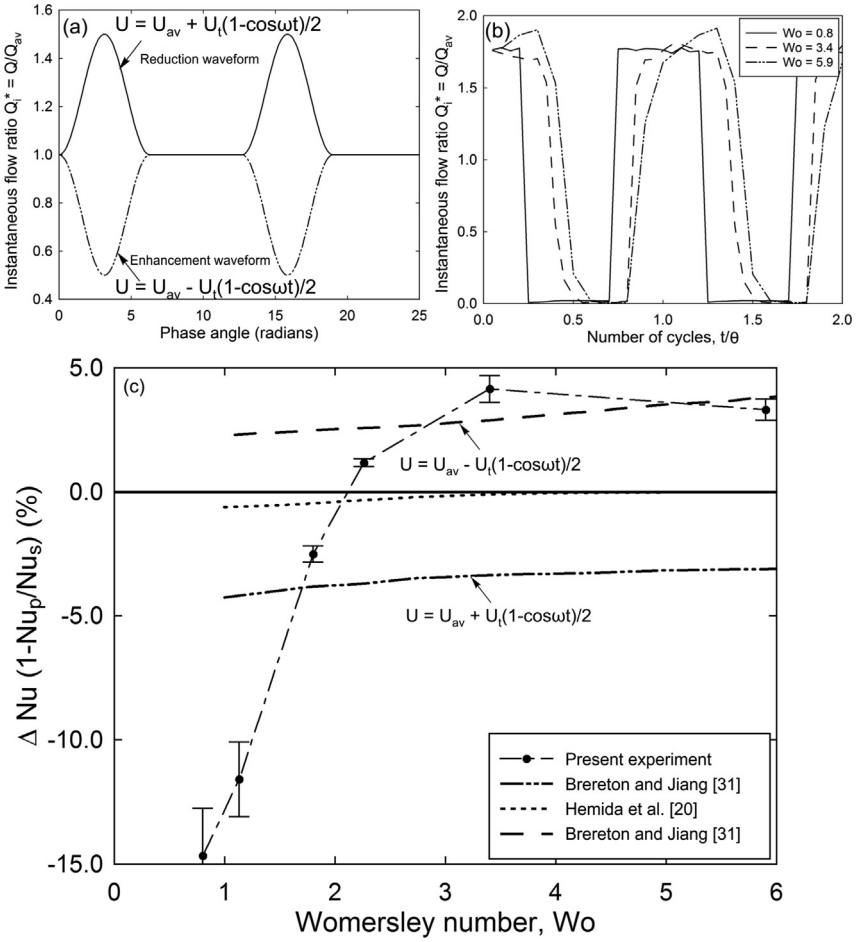

Fig. 7. (a) Waveform used in Ref. [31] (b) Waveforms used in the present work (c) Deviation of mean relative *Nu* from steady-state value for different *Wo*; For comparison, results from literature are also plotted along with the present experimental data; Present experiment ($Pr \approx 5.5$, amplitude ratio ≈ 0.92, thermally developing); Brereton and Jiang ($Pr \approx 7$, amplitude ratio ≈ 0.5, thermally developed) [31]; Hemida et al. ($Pr \approx 5$, amplitude ratio ≈ 0.4, thermally developing) [20].

4. Summary and conclusions

In this paper, effect of imposed pulsations on laminar thermally developing single-phase flow and heat transfer in a square mini-channel is studied. Frequency is the only variable, while amplitude of flow pulsations and average flow Reynolds number are kept constant. When single-phase flow is perturbed with externally imposed oscillations at lower frequency of $Wo = 0.8$ ($f = 0.05$ Hz), when the diffusional time scale is comparable with the time scale of imposed fluctuations, convection becomes insignificant and heat transfer deteriorates. However, for convection dominant pulsating flow ($Wo = 3.4$ and 5.9) only marginal enhancement, having practically no significance for engineering applications, is observed. In fact, at very low frequency of the flow pulsation, time averaged heat transfer gets deteriorated. In essence, during pulsatile flows studied in the present work, average heat transfer coefficient is related to average flow rate. In contrast to steady flows where the entire physics of convective heat transfer can be effectively scaled with *Re* and *Pr*, in pulsatile flows, the relationship of *Nu* with *Pr* and *Wo* is much more complicated. Universal formulation with simple power law type correlations seem to be elusive due to complex interplay of thermo-physical properties and the associated time scales.

Acknowledgments

Financial grants for undertaking this research work, obtained from the Indo-French Center for Promotion of Advanced Research (IFCPAR Grant number 4408-1), are gratefully acknowledged. InfraRed Thermography facility was developed by the grants received from Department of Science and Technology, Government of India.

References

[1] E.G. Richardson, E. Tyler, The transverse velocity gradient near the mouths of pipes in which an alternating or continuous flow of air is established, Proc. Phys. Soc. 42 (231) (1929) 1–15.
[2] J.R. Womersley, Method for the calculation of velocity rate of flow and viscous drag in arteries when the pressure gradient is known, J. Physiol. 127 (1955) 553–563.
[3] D.A. McDonald, The relation of pulsatile pressure to flow in arteries, J. Physiol. 127 (1955) 533–552.
[4] J.F. Hale, D.A. McDonald, J.R. Womersley, Velocity profiles of oscillating arterial flow, with some calculations of viscous drag and the Reynolds number, J. Physiol. 128 (1955) 629–640.
[5] S. Uchida, The pulsating viscous flow superposed on the steady laminar motion of incompressible fluid in a circular pipe, ZAMP 7 (1956) 403–422.
[6] A. Yakhot, M. Arad, G. Ben-Dor, Numerical investigation of laminar pulsating flow in a rectangular duct, Int. J. Numer. Methods Fluids 29 (1999) 935–950.
[7] W. Chang, G. Pu-zhen, T. Si-chao, X. Chao, Theoretical analysis of phase-lag in low frequency laminar pulsating flow, Prog. Nucl. Energy 58 (2012) 45–51.
[8] S. Ray, B. Ünsal, F. Durst, Development length of sinusoidally pulsating laminar pipe flows in moderate and high Reynolds number regimes, Int. J. Heat Fluid Flow 37 (2012) 167–176.
[9] R. Siegel, M. Perlmutter, Heat transfer for pulsating laminar duct flow, ASME J. Heat Transf. (May, 1962) 111–123.
[10] E.M. Phillips, S.H. Chiang, Pulsatile Newtonian friction losses in a rigid tube, Int. J. Eng. Sci. 11 (1973) 579–589.
[11] T. Muto, K. Nakane, Unsteady flow in circular tube, Bull. JSME 23 (186) (1980) 1990–1996.
[12] Y. Kita, T. Hayashi, K. Hirose, Heat transfer in pulsating laminar flow in a pipe, Bull. JSME 25 (200) (1982) 217–224.
[13] R. Creff, J. Batina, P. Andre, V.S. Karunanithi, Numerical model for dynamic and thermal developments of a pulsed laminar ducted flow, Numer. Heat Transf. 6 (1983) 173–188.
[14] R. Creff, P. Andre, J. Batina, Dynamic and convective results for a developing laminar unsteady flow, Int. J. Numer. Methods Fluids 5 (1985) 745–760.
[15] A.A. Al-Haddad, N. Al-Binally, Prediction of heat transfer coefficient in pulsating flow, Int. J. Heat Fluid Flow 10 (2) (1989) 131–133.
[16] R. Siegel, Influence of oscillation-induced diffusion on heat transfer in a uniformly heated channel, Trans. ASME J. Heat Transf. 109 (1987) 224–247.
[17] H.W. Cho, J.M. Hyun, Numerical solutions of pulsating flow and heat transfer characteristics in a pipe, Int. J. Heat Fluid Flow 11 (4) (1990) 321–330.
[18] S.Y. Kim, B.H. Kang, J.M. Hyun, Heat transfer in the thermally developing region of a pulsating channel flow, Int. J. Heat Mass Transf. 36 (17) (1993) 4257–4266.
[19] Z. Guo, J.H. Sung, Analysis of the Nusselt number in pulsating pipe flow, Int. J. Heat Mass Transf. 40 (10) (1997) 2486–2489.
[20] H.N. Hemida, M.N. Sabry, A. Abdel-Rahim, H. Mansour, Theoretical analysis of heat transfer in laminar pulsating flow, Int. J. Heat Mass Transf. 45 (2002) 1767–1780.
[21] Z. Jun, Z. Danling, W. Ping, G. Hong, An experimental study of heat transfer enhancement with a pulsating flow, Heat Transf. Asian Res. 33 (2004) 279–286.
[22] J. Yu, Z. Li, T.S. Zhao, An analytical study of pulsating laminar heat convection in a circular tube with constant heat flux, Int. J. Heat Mass Transf. 47 (2004) 5297–5301.
[23] H. Chattopadhyay, F. Durst, S. Ray, Analysis of heat transfer in simultaneously developing pulsating laminar flow in pipe with constant wall temperature, Int. Commun. Heat Mass Transf. 33 (2006) 475–481.
[24] P. Bouvier, P. Stouffs, J.P. Bardon, Experimental study of heat transfer in oscillating flow, Int. J. Heat Mass Transf. 48 (2005) 2473–2482.
[25] D.A. Nield, A.V. Kuznetsov, Forced convection with laminar pulsating flow in a channel or tube, Int. J. Therm. Sci. 46 (2007) 551–560.
[26] B. Mehta, S. Khandekar, Effect of Periodic Pulsations on Heat Transfer in Simultaneously Developing Laminar Flows: A Numerical Study, IHTC 14, Washington DC, USA, 2010. IHTC14-22519.
[27] M. Rahgoshay, A.A. Ranjbar, A. Ramiar, Laminar pulsating flow of nanofluids in a circular tube with isothermal wall, Int. Commun. Heat Mass Transf. 39 (2012) 463–469.
[28] M. Faghri, K. Javadani, Heat transfer with laminar pulsating flow in a pipe, Lett. Heat Mass Transf. 6 (1979) 259–270.
[29] B. Ünsal, S. Ray, F. Durst, Ö. Ertunç, Pulsating laminar pipe flows with sinusoidal mass flux variations, Fluid Dyn. Res. 37 (2005) 317–333.
[30] H.W. Wu, R.F. Lay, C.T. Lau, W.J. Wu, Turbulent flow field and heat transfer in a heated circular channel under a reciprocating motion, Heat Mass Transf. 40 (2003) 769–778.
[31] G.J. Brereton, Y. Jiang, Convective heat transfer in unsteady laminar parallel flows, Phys. Fluids 18 (2006) 1–15, 103602.